The Thermodynamics of Polyamide−DNA Recognition: Hairpin Polyamide Binding in the Minor Groove of Duplex DNA†

Daniel S. Pilch,*,‡,§ Nataša Poklar,||,⊥ Eldon E. Baird,# Peter B. Dervan,# and Kenneth J. Breslauer*,§,||

Department of Pharmacology, University of Medicine and Dentistry of New Jersey, Robert Wood Johnson Medical School, Piscataway, New Jersey 08854, Department of Chemistry, Rutgers-The State University of New Jersey, Piscataway, New Jersey 08854-8087, The Cancer Institute of New Jersey, New Brunswick, New Jersey 08901, and Division of Chemistry and Chemical Engineering, California Institute of Technology, Pasadena, California 91125

Received November 4, 1998

ABSTRACT: Crescent-shaped synthetic ligands containing aromatic amino acids have been designed for specific recognition of predetermined DNA sequences in the minor groove of DNA. Simple rules have been developed that relate the side-by-side pairings of Imidazole (Im) and Pyrrole (Py) amino acids to their predicted target DNA sequences. We report here thermodynamic characterization of the DNA-binding properties of the six-ring hairpin polyamide, ImImPy-γ-PyPyPy-β-Dp (where γ = γ-aminobutyric acid, β = β-alanine, and Dp = dimethylaminopropylamide). Our data reveal that, at 20 °C, this ligand binds with a relatively modest 1.8-fold preference for the designated match site, 5′-TGGTA-3′, over the single base pair mismatch site, 5′-TGTTA-3′. By contrast, we find that the ligand exhibits a 102-fold greater affinity for its designated match site relative to the double base pair mismatch site, 5′-TATTA-3′. These results demonstrate that the energetic cost of binding to a double mismatch site is not necessarily equal to twice the energetic cost of binding to a single mismatch site. Our calorimetrically measured binding enthalpies and calculated entropy data at 20 °C reveal the ligand sequence specificity to be enthalpic in origin. We have compared the DNA-binding properties of ImImPy-γ-PyPyPy-β-Dp with the hairpin polyamide, ImPyPy-γ-PyPyPy-β-Dp (an Im → Py "mutant"). Our data reveal that both ligands exhibit high affinities for their designated match sites, consistent with the Dervan pairing rules. Our data also reveal that, relative to their corresponding single mismatch sites, ImImPy-γ-PyPyPy-β-Dp is less selective than ImPyPy-γ-PyPyPy-β-Dp for its designated match site. This result suggests, at least in this case, that enhanced binding affinity can be accompanied by some loss in sequence specificity. Such systematic comparative studies allow us to begin to establish the thermodynamic database required for the rational design of synthetic polyamides with predictable DNA-binding affinities and specificities.

Polyamides containing three aromatic amino acids, *N*-methylpyrrole (Py),[1] *N*-methylimidazole (Im), and *N*-methyl-3-hydroxypyrrole (Hp), are synthetic ligands that bind to predetermined sequences of DNA according to simple pairing rules (*1*, *2*). Consequently, these ligands may be useful for the regulation of gene expression. For sequence-specific recognition of DNA through the minor groove, a polyamide pairing of Im opposite Py (Im/Py) targets a G·C base pair, while a Py/Im polyamide pair targets a C·G base pair (*1*, *2*). A Py/Py polyamide combination is degenerate, targeting both T·A and A·T base pairs (*1*−*4*). However, a Hp/Py polyamide pair discriminates T·A from A·T base pairs, and both from G·C or C·G base pairs (*5*). The structure of each of these ring pairings opposite its cognate base pair has been characterized by NMR (*6*−*8*) and by high-resolution X-ray structure analysis (*9*−*11*). These structures reveal a pattern of specific hydrogen bonds between the polyamide and the edges of the Watson−Crick base pairs, as well as an ensemble of van der Waals contacts between the polyamide and the walls of the DNA minor groove. This impressive structural picture of polyamide−DNA complexes needs to be complemented by energetic data, including dissection of the binding free energies into their enthalpic and entropic contributions. Such thermodynamic data on families of matched and mismatched polyamide−DNA complexes are essential for understanding the nature and relative strengths of the molecular forces that dictate the observed DNA affinities and specificities of the polyamides. On a practical level, thermodynamic data are required to establish a database that can be used to predict, over a range of conditions, the relative affinity of a given polyamide for a targeted DNA site (e.g., the match site) versus binding to possible competing secondary or tertiary sites (e.g. single and double mismatch sites).

† This work was supported by National Institutes of Health Grants GM-23509 (K.J.B.), GM-34469 (K.J.B.), CA-47995 (K.J.B.), CA-77433 (D.S.P.), and GM-27681 (P.B.D.) and a Howard Hughes Medical Institute predoctoral fellowship to E.E.B.

* To whom correspondence should be addressed.
‡ UMDNJ-Robert Wood Johnson Medical School.
§ Cancer Institute of New Jersey.
|| Rutgers University.
⊥ Present address: Faculty of Chemistry and Chemical Technology, University of Ljubljana, 1001 Ljubljana, Slovenia.
California Institute of Technology.

[1] Abbreviations: Im, *N*-methylimidazole; Py, *N*-methylpyrrole; Hp, *N*-methyl-3-hydroxypyrrole; β, β-alanine; γ, γ-aminobutyric acid; Dp, dimethylaminopropylamide; r_{Dup}, [total ligand] to [duplex] ratio; T_m, melting temperature; CD, circular dichroism; DSC, differential scanning calorimetry.

10.1021/bi982628g CCC: $18.00
Published on Web 01/27/1999

Hairpin polyamides have pronounced enhancements in both binding affinity and specificity relative to the dimer (*12*−*16*), achieving affinities and specificities comparable to DNA-binding proteins. Recently, we have shown that the hairpin polyamide ImPyPy-γ-PyPyPy-β-Dp exhibits a ~2−3 kcal/mol binding preference for its designated match site, 5′-TGTTA-3′, relative to its single base pair mismatch sites, 5′-TGGTA-3′ and 5′-TATTA-3′, with this sequence specificity being *enthalpic in origin* (*17*). This sequence-specific discrimination is consistent with the Dervan pairing rules being governed by enthalpically favorable polyamide−DNA interactions, perhaps including the formation of specific hydrogen bonds between the ligand and the target DNA sequence, as revealed in the structural studies (*6*−*11*). In addition to the family of 5′-(A,T)G(A,T)$_3$-3′ match sequences (such as 5′-TGTTA-3′ noted above), we also have explored the recognition of 5′-(A,T)GG(A,T)$_2$-3′ sequences by hairpin polyamides containing neighboring Im rings (*14*, *15*). As predicted by the pairing rules, the ImImPy-γ-PyPyPy-β-Dp hairpin polyamide binds a designated 5′-TGGTT-3′ match site with a 50-fold and 100-fold greater affinity than the single base pair mismatch sites, 5′-TGTTA-3′ and 5′-GGGTA-3′, respectively (*14*). This demonstration of the specific recognition of DNA sequences containing contiguous G·C base pairs has expanded the repertoire of sequences that can be targeted by such designer DNA-binding ligands.

Footprinting and affinity cleaving studies have provided a wealth of information regarding the DNA sequence affinities and orientations of Im-Py polyamides (*18*). Despite the richness of this database, little is known of the thermodynamic driving forces that govern the binding events. Such thermodynamic information should prove to be particularly useful in gene inhibition experiments, where both affinity (subnanomolar K_D) and specificity (ΔK_D) are of premium value, by providing a basis for the rational design of ligand motifs and solution conditions that should maximize ligand targetting for the primary, match DNA site, while minimizing ligand binding to secondary and tertiary mismatch sites.

In this paper, we report calorimetric and spectroscopic studies designed to characterize the binding enthalpy and entropy of the hairpin polyamide, ImImPy-γ-PyPyPy-β-Dp, to three 11-mer DNA duplexes, whose base sequences are presented in Figure 1. The central 5 base pair sequence of one of the three duplexes (duplex **2**) is 5′-TGGTA-3′, which represents a match site for ImImPy-γ-PyPyPy-β-Dp binding, as defined by the pairing rules and by footprinting studies. Duplex **1** contains a single base pair change in the match site to produce the 5′-TGTTA-3′ single mismatch site, while duplex **3** contains a double base pair change in the match site to produce the 5′-TATTA-3′ double mismatch site. A thermodynamic comparison of ImImPy-γ-PyPyPy-β-Dp and ImPyPy-γ-PyPyPy-β-Dp binding to these three DNA sites is reported. We also discuss potential macroscopic−microscopic correlations by comparing the differential binding properties we measure with the NMR-derived structure of a hairpin polyamide−DNA complex (*19*).

MATERIALS AND METHODS

Oligonucleotide Synthesis and Characterization. Oligomers were synthesized and purified as previously described (*17*). Molar extinction coefficients (ϵ) for the single-stranded

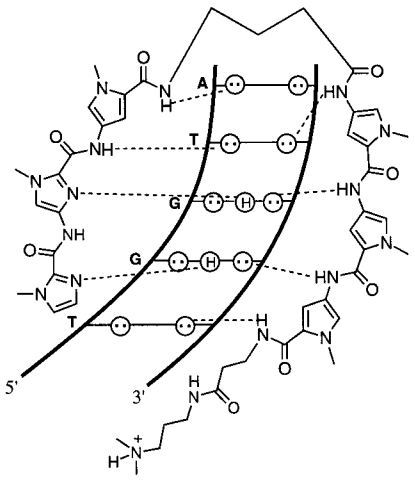

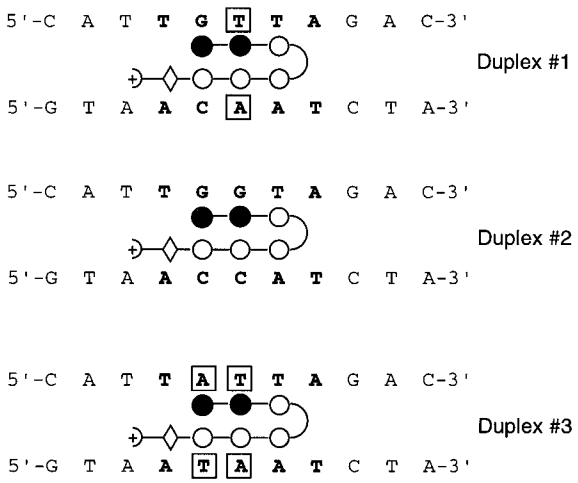

FIGURE 1: (Top) Model for the complex formed between the hairpin polyamide ImImPy-γ-PyPyPy-β-Dp and the 5′-TGGTA-3′ match site of duplex **2**. Circles with dots represent lone electron pairs of either N3 of adenine, O2 of thymine, or O2 of cytosine. Circles containing an H represent the 2-amino proton of guanine. Putative hydrogen bonds are illustrated by dotted lines. (Bottom) Base sequences of the three 11-mer DNA duplexes used in this study (denoted as duplexes **1**, **2**, and **3**). The central five base pair binding sites of each duplex are presented in boldface type. The boxes indicate the bases pairs in duplexes **1** and **3** that have been changed relative to the match duplex **2**. Schematic binding models of putative complexes between the hairpin polyamide and each duplex. The imidazole and pyrrole rings are represented as shaded and unshaded spheres, respectively, while the β-alanine residue is represented as an unshaded diamond.

oligonucleotides at 260 nm and 25 °C [in units of ((mol strand)/L)$^{-1}$ cm^{-1}] were determined in 10 mM sodium cacodylate (pH 7.0) by enzymatic degradation and subsequent phosphate analysis (*20*). The following ϵ values were so obtained: 96900 for d(CATTGTTAGAC); 97400 for d(GTCTAACAATG); 94300 for d(CATTGGTAGAC); 91500 for d(GTCTACCAATG); 92000 for d(CATTATTAGAC); and 104700 for d(GTCTAATAATG).

Hairpin Polyamide Synthesis and Characterization. The polyamide, ImImPy-γ-PyPyPy-β-Dp (Figure 1), was prepared by machine-assisted solid-phase protocols and characterized by a combination of ^{1}H NMR, analytical HPLC, and matrix-assisted laser desorption ionization time-of-flight mass spectrometry (MALDI-TOF), with the details described elsewhere (*21*). Concentrations of ImImPy-γ-PyPyPy-β-Dp

were determined spectrophotometrically using an extinction coefficient of 55200 ± 1000 cm^{-1} M^{-1} at 311 nm and 25 °C, as determined by dry weight and verified by the slope of a linear plot of absorbance versus ligand concentration.

Buffer Conditions. All of the spectroscopic and calorimetric experiments were conducted in 10 mM sodium cacodylate (pH 6.9), 10 mM KCl, 10 mM $MgCl_2$, and 5 mM $CaCl_2$. These buffer conditions were chosen to match as closely as possible those used by the Dervan group in their quantitative footprinting studies on the ImImPy-γ-PyPyPy-β-Dp and ImPyPy-γ-PyPyPy-β-Dp hairpin polyamides (*12*−*14*). We used 10 mM sodium cacodylate in place of the 10 mM Tris·HCl employed by the Dervan group, since the large temperature dependence of the pK_a for Tris·HCl (−0.031 ΔpK_a/°C) makes it poorly suited for thermal denaturation experiments.

UV Absorption Spectrophotometry. Absorbance versus temperature profiles were measured at 260 nm using a computer-interfaced Perkin-Elmer model Lambda 4C spectrophotometer equipped with a thermoelectrically controlled cell holder and a cell path length of 1 cm. The heating rate in all experiments was 0.5 °C/min. For each optically detected transition, the melting temperature (T_m) was determined as described previously (*22*, *23*). The DNA concentration was 5 μM in duplex, while the ImImPy-γ-PyPyPy-β-Dp concentration ranged from 0 to 15 μM.

Circular Dichroism (CD) Spectropolarimetry. All CD measurements were performed on an AVIV Model 60DS Spectropolarimeter (Aviv Associates; Lakewood, NJ) equipped with a thermoelectrically controlled cell holder and cell path length of 1 cm. Isothermal ImImPy-γ-PyPyPy-β-Dp titrations were performed at 20 °C by incrementally adding 5−20 μL aliquots of 250−300 μM ligand into a 2 mL solution of 5 μM duplex. After each addition, the CD spectrum was recorded from 220 to 380 nm, with an averaging time of 3 s. The final CD spectra were normalized to reflect equimolar concentrations of duplex.

Isothermal Stopped-Flow Mixing Microcalorimetry. Isothermal calorimetric measurements were performed using an all tantalum, differential, stopped-flow, heat conduction microcalorimeter (model DSFC-100, Commonwealth Technology, Inc.; Alexandria, VA), developed by Mudd and Berger (*24*, *25*). In a typical experiment, the reaction was initiated by a microprocessor-controlled stepping motor that activates a syringe drive which delivers, within 0.6 s, 80 μL of each reagent (25 μM in duplex and/or polyamide) into tantalum mixing chambers, with distilled water being used in the reference mixing chamber. A delay of 200 s was used between each injection/reaction. Each reaction generated a heat burst curve (microjoules per second versus second), with the area under the curve being determined by integration to obtain the heat for that reaction, which ranged from 42 to 92 μJ compared with polyamide dilution heats of 32 μJ. Note that none of the 11-mer duplexes studied here exhibited measurable heats of dilution. The calorimeter was calibrated chemically by measuring the heat associated with a 1:2 dilution of 10 mM NaCl (*26*, *27*).

RESULTS AND DISCUSSION

ImImPy-γ-PyPyPy-β-Dp Binds to and Enhances the Thermal Stability of Each DNA Duplex in a Manner that Is Sensitive to the Target Sequence. UV melting experiments were conducted in the absence and presence of ligand to assess the impact, if any, of ImImPy-γ-PyPyPy-β-Dp on the thermal stabilities of the three 11-mer DNA duplexes studied here. The resulting melting profiles are shown in Figure 2. Note that, as the [total ligand] to [duplex] ratio (r_{Dup}) increases from 0 to 1.0, the thermal stabilities of all three host duplexes increase concomitantly. Polyamide-to-duplex ratios above 1.0 result in only marginal increases in the T_m of either duplex (data not shown), an observation which may reflect some nonspecific, secondary binding to the target duplexes at high polyamide concentrations.

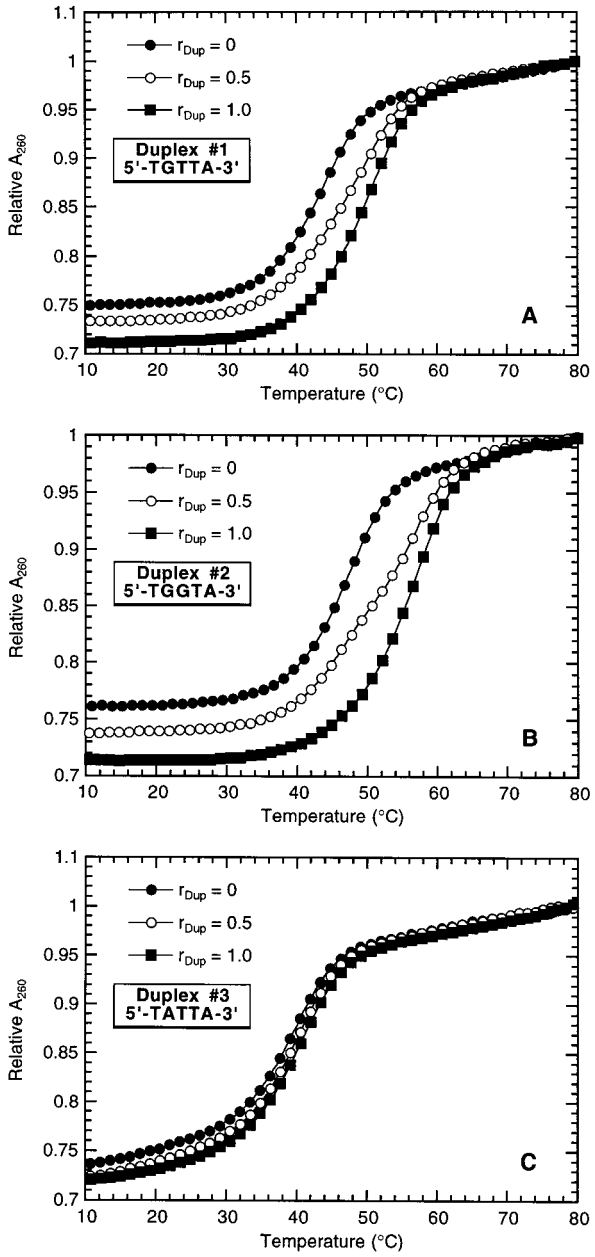

FIGURE 2: UV melting profiles at 260 nm for duplexes **1** (A), **2** (B), and **3** (C) and their ImImPy-γ-PyPyPy-β-Dp complexes at the indicated ratios of [total ligand] to [duplex] {r_{Dup}}. Solution conditions are 10 mM sodium cacodylate (pH 6.9), 10 mM KCl, 10 mM $MgCl_2$, and 5 mM $CaCl_2$. For clarity of presentation, the melting curves for a given duplex and its ImImPy-γ-PyPyPy-β-Dp complexes are normalized so as to produce identical absorbances at 80 °C.

The ImImPy-γ-PyPyPy-β-Dp-induced changes in duplex thermal stability noted above are consistent with the ligand binding to the three 11-mer duplexes, with a preference for the duplex versus the single-stranded state (*28*, *29*). The extent of this thermal enhancement follows the hierarchy duplex **2** (5′-TGGTA-3′) > duplex **1** (5′-TGTTA-3′) > duplex **3** (5′-TATTA-3′). At an r_{Dup} ratio of 1.0, ImImPy-γ-PyPyPy-β-Dp binding increases the thermal stabilities (T_m) of duplex **2** (Figure 2B), duplex **1** (Figure 2A), and duplex **3** (Figure 2C) by approximately 9, 6, and 1 °C, respectively (see Table 3 below). Thus, relative to complexation with the 5′-TGGTA-3′ *match* site, binding of the hairpin polyamide to the 5′-TGTTA-3′ *single mismatch* site and the 5′-TATTA-3′ *double mismatch* site reduces the extent of ligand-induced enhancement in duplex thermal stability by 3 and 8 °C, respectively. In other words, as measured by differences in ΔT_m ($\Delta\Delta T_m$), the hairpin polyamide is able to distinguish between duplex targets that differ by as little as one base pair, with the extent to which the target sequence deviates from the sequence of the match site being correlated with the magnitude of $\Delta\Delta T_m$.

CD Reveals that the Hairpin Polyamide Binds to All Three Duplexes with a Common Stoichiometry of One Ligand Molecule per Duplex, and with Isoelliptic Points Consistent with a Single Binding Motif. In addition to the UV melting studies described above, CD spectropolarimetry provides a second means for detecting and characterizing the DNA binding of the hairpin polyamide. Figure 3 shows the CD spectra from 220 to 380 nm obtained by incremental titration at 20 °C of ImImPy-γ-PyPyPy-β-Dp into a solution of either duplex **1** (Figure 3A), duplex **2** (Figure 3B), or duplex **3** (Figure 3C). In the DNA-absorbing wavelength region (220−300 nm), each family of CD spectra shares two isoelliptic points. These isoelliptic points are observed at 244 and 267 nm for the duplex **1** titration (Figure 3A), at 245 and 268 nm for the duplex **2** titration (Figure 3B), and at 242 and 271 nm for the duplex **3** titration (Figure 3C). The presence of distinct pairs of isoelliptic points for the three duplexes is consistent with a single, CD-detectable, ImImPy-γ-PyPyPy-β-Dp binding event when each duplex serves as the host.

Neither the free hairpin polyamide (not shown) nor the free duplexes (Figure 3) exhibit CD signals in the ligand-absorbing 300−380 nm wavelength region. However, upon addition of the ligand to a solution of any one of the three duplexes, a substantial CD signal arises in this wavelength range. This induced CD signal is indicative of interactions between ImImPy-γ-PyPyPy-β-Dp and each of the host duplexes and can be used, as described below, to detect and to monitor the *CD-active* DNA-binding mode.

Titration curves at 325 nm, extracted from the CD spectra shown in Figure 3, are presented in Figure 4. The total ligand concentration that corresponds to the inflection point observed for ImImPy-γ-PyPyPy-β-Dp binding to each of the three host duplexes provides an estimate of the ligand−duplex stoichiometry. Inspection of Figure 4 reveals that the inflection points for ImImPy-γ-PyPyPy-β-Dp binding to each of the three host duplexes correspond to a total ligand concentration of ~5 μM. Recall from the Material and Methods that the total duplex concentration in each of the CD titrations depicted in Figure 4 is 5 μM. Thus, ImImPy-γ-PyPyPy-β-Dp binds to each host duplex with an apparent

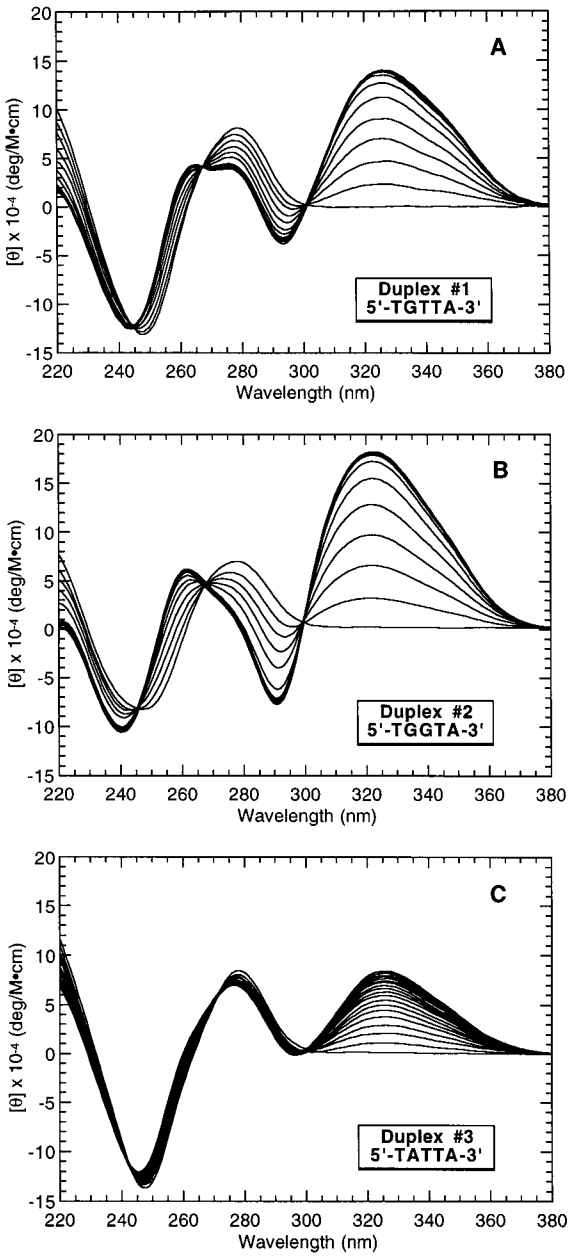

FIGURE 3: CD titrations at 20 °C of either duplex **1** (A), duplex **2** (B), or duplex **3** (C) with ImImPy-γ-PyPyPy-β-Dp. Solution conditions are as described in the legend to Figure 2. Molar ellipticities, [θ], are in units of deg M^{-1} cm^{-1}, where M refers to moles of DNA strand per liter.

stoichiometry of approximately one ligand molecule per duplex. Further inspection of Figure 4 reveals the curvature of the titration curves for duplexes **1** and **2** to be substantially sharper than the curvature of the corresponding curve for duplex **3**. This difference in curvature is consistent with the ligand binding to duplexes **1** and **2** with a greater affinity than it binds to duplex **3**, a correlation that is substantiated by the ligand-binding constants we calculate at 20 °C (see below).

Induced CD Titration Profiles Reveal that the Hairpin Polyamide Binds to the 5′-TGGTA-3′ Match Site with Only a 1.7-Fold Greater Affinity than It Binds to the 5′-TGTTA-3′ Single Mismatch Site, but with a 46-Fold Greater Affinity than it Binds to the 5′-TATTA-3′ Double Mismatch Site. By fitting the induced CD titration curves shown in Figure 4,

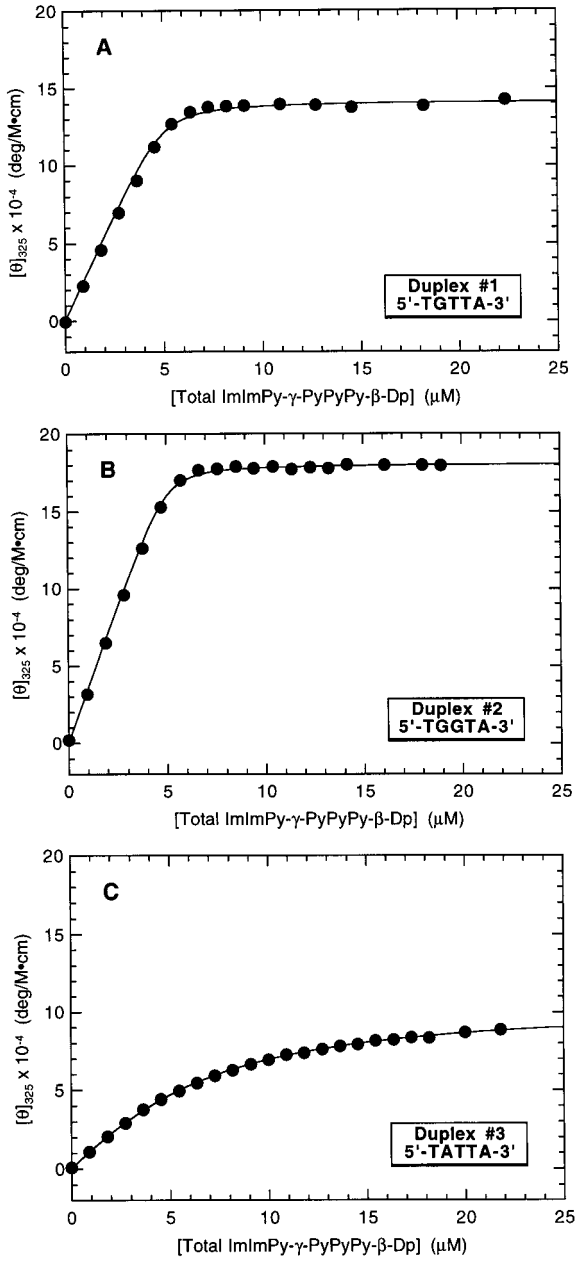

FIGURE 4: Molar ellipticities at 325 nm ($[\theta]_{325}$) versus total ligand concentration for the titration of either duplex **1** (A), duplex **2** (B), or duplex **3** (C) with ImImPy-γ-PyPyPy-β-Dp. The solid lines represent the best fits of the data using eq 1. Solution conditions and $[\theta]$ are as defined in the legends to Figures 2 and 3, respectively.

we have derived ligand−duplex association constants at 20 °C (K). This fitting was accomplished using eq 1, which is predicated on formation of a 1:1 complex.

$$[\theta] = \frac{[\theta]_\infty}{2}\left\{\left([\mathrm{D}]_\mathrm{T} + [\mathrm{L}]_\mathrm{T} + \frac{1}{K_{20}^{\mathrm{fit}}}\right) - \sqrt{\left([\mathrm{D}]_\mathrm{T} + [\mathrm{L}]_\mathrm{T} + \frac{1}{K_{20}^{\mathrm{fit}}}\right)^2 - 4[\mathrm{D}]_\mathrm{T}[\mathrm{L}]_\mathrm{T}}\right\} \quad (1)$$

where $[\theta]_\infty$ is the induced CD of the ligand at an infinite r_{Dup} ratio, $[\mathrm{D}]_\mathrm{T}$ is the total duplex concentration, and $[\mathrm{L}]_\mathrm{T}$ is the total ligand concentration. The solid lines in Figure 4 represent the best fits using eq 1. Note that these fits are associated with correlation (R) factors of >0.998, an observation which supports the validity of the assumption of a 1:1 stoichiometry, as well as our use of this equation to fit the induced CD data. The K values derived from this analysis are listed in Table 1. Inspection of these data reveals that the apparent binding affinities of the hairpin polyamide follow the hierarchy, match duplex **2** (5′-TGGTA-3′) > single mismatch duplex **1** (5′-TGTTA-3′) > double mismatch duplex **3** (5′-TATTA-3′). Note the agreement between this hierarchy and that noted above for binding-induced enhancement in duplex thermal stability. Thus, in this case, the relative extent to which ImImPy-γ-PyPyPy-β-Dp binding thermally stabilizes the target duplex is correlated with its relative binding affinity.

Table 1: CD-Derived Binding Affinities of ImImPy-γ-PyPyPy-β-Dp for the Three 11-mer DNA Duplexes at 20 °C[a]

duplex	K_{20}^{fit} [b] (M^{-1})
1 (5′-TGTTA-3′)	$(7.5 \pm 1.9) \times 10^6$
2 (5′-TGGTA-3′)	$(1.3 \pm 0.2) \times 10^7$
3 (5′-TATTA-3′)	$(2.8 \pm 0.1) \times 10^5$

[a] Solution conditions were 10 mM sodium cacodylate (pH 6.9), 10 mM KCl, 10 mM $MgCl_2$, and 5 mM $CaCl_2$. [b] Binding constants at 20 °C (K_{20}^{fit}) were determined by fitting the induced CD titration curves shown in Figure 4 with eq 1. The indicated uncertainties reflect the standard errors resulting from the fitting analyses.

Inspection of the binding constant, K, data in Table 1 reveals that the polyamide exhibits only a ~1.7-fold greater affinity for the 5′-TGGTA-3′ match site of duplex **2** [$K = (1.3 \pm 0.2) \times 10^7\ \mathrm{M}^{-1}$] relative to the 5′-TGTTA-3′ single mismatch site of duplex **1** [$K = (7.5 \pm 1.9) \times 10^6\ \mathrm{M}^{-1}$]. In other words, the ImImPy-γ-PyPyPy-β-Dp ligand does not strongly discriminate between its match and single mismatch sites. By contrast, we previously found the differential affinity of the ImPyPy-γ-PyPyPy-β-Dp polyamide for its match and single mismatch sites to be ~88-fold. *Thus, although the Py to Im alteration in the ligand increases its binding affinity for the 5′-TGGTA-3′ match site, it also reduces its binding selectivity for the match site relative to a single mismatch site.*

Further inspection of the data in Table 1 reveals the binding affinity of the ImImPy-γ-PyPyPy-β-Dp ligand for the double mismatch site, 5′-TATTA-3′, of duplex **3** to be $(2.8 \pm 0.1) \times 10^5\ \mathrm{M}^{-1}$ compared to a ligand-binding affinity of $(1.3 \pm 0.2) \times 10^7\ \mathrm{M}^{-1}$ for complexation to the match site, 5′-TGGTA-3′, of duplex **2**. Thus, the ligand exhibits a 46-fold preference ($1.3 \times 10^7/2.8 \times 10^5$) for the match site versus the double mismatch site. This result is interesting for several reasons. First, it provides a quantification of the free energy penalty associated with this double mispairing. Further, the significant 46-fold penalty occurs despite the fact that the double mismatch site (5′-TATTA-3′) presents the hairpin polyamide with a sterically unobstructed minor groove [the absence of a guanine exocyclic amino group]. In this connection, in a previous study (*17*), we found that the hairpin polyamide, ImPyPy-γ-PyPyPy-β-Dp (an Im → Py "mutant" of the ligand studied here), binds the sterically unobstructed 5′-TATTA-3′ site with a ~17-fold greater affinity than that exhibited by the ImImPy-γ-PyPyPy-β-Dp ligand. Another point worthy of emphasis is that, relative to the match site, the double mismatch site is a much poorer ligand receptor (a 46-fold decrease in ligand binding) than the single mismatch site (only a 1.7-fold decrease in ligand

binding). Stated somewhat differently, relative to ligand binding to the match site, the double mismatch does not simply impose twice the energetic penalty as that imposed by the single mismatch. Thus, the energetic consequences of the mismatches are far from additive. This nonadditivity represents an important observation in terms of the development and application of the thermodynamic database required for the design of polyamides with predictable DNA-binding affinities and specificities.

Structural Interpretation of the Thermodynamic Data. A recent NMR study on the complex of ImPyPy-γ-PyPyPy-β-Dp bound in the minor groove of the d(GCCTGTTAGCG)·d(CGCTAACAGGC) duplex provides us with a structural context in which to interpret the similarity in ImImPy-γ-PyPyPy-β-Dp-binding affinity for its 5′-TGGTA-3′ match site and for its 5′-TGTTA-3′ single mismatch site (*19*). The 5′-TGTTA-3′ binding site in the NMR study is the same as that present in duplex **1** of this study, while the hairpin polyamide is the same as that studied here except that it contains one rather than two Im residues.

The structural picture to emerge from the NMR study invokes the formation of two imidazole(N)−(amino H2)-guanine hydrogen bonds and one amide-(O2)thymine hydrogen bond when ImImPy-γ-PyPyPy-β-Dp is complexed with the 5′-TGGTA-3′ match site of duplex **2**. By extension, it is reasonable to suggest that when the ligand is complexed with the 5′-TGTTA-3′ single mismatch site of duplex **1**, the polyamide would be unable to form one of the two imidazole(N)−(amino H2)guanine hydrogen bonds. This loss of a hydrogen bond, however, may be compensated by formation of a hydrogen bond between the amide located between the Im−Im neighboring pair and the O2 atom of the complementary thymine residue at position 3. An alternative explanation for the similar affinities with which ImImPy-γ-PyPyPy-β-Dp binds to both the match and single mismatch sites (5′-TGGTA-3′ versus 5′-TGTTA-3′) invokes the possibility that the hydrogen bond formed between the *terminal* Im moiety and the 2-amino group of its target guanine residue stabilizes the ligand−duplex complex to a substantially greater extent than the hydrogen bond formed between the penultimate ("*internal*") Im moiety and the 2-amino group of its target guanine residue. As discussed in the next section, either of these two structural explanations are consistent with the virtually identical ligand-binding enthalpies exhibited by duplexes **2** and **1**. We are aware, however, that other microscopic interpretations of our macroscopic data are possible, including those involving energetic contributions from differential solvation, as well as the possibility of altered binding motifs to mismatched sites. We simply offer the microscopic interpretations presented here as a basis for further discussion.

ImImPy-γ-PyPyPy-β-Dp Binding to the 5′-TGGTA-3′ Match Site and to the 5′-TGTTA-3′ Single Mismatch Site Is Enthalpically Similar, while Being Enthalpically More Favorable than Ligand Binding to the 5′-TATTA-3′ Double Mismatch Site. Isothermal, stopped-flow mixing calorimetry was used to measure the binding enthalpies (ΔH_b) for ImImPy-γ-PyPyPy-β-Dp complexation with the three 11-mer DNA duplexes studied here. The resulting ΔH_b values are listed in Table 2. Inspection of these data reveals that the enthalpies for hairpin polyamide binding to duplex **2**, which contains the 5′-TGGTA-3′ match site, and to duplex **1**, which contains the 5′-TGTTA-3′ single mismatch site, are −6.9 and −6.6 kcal/mol, respectively, values that are essentially indistinguishable. Thus, ImImPy-γ-PyPyPy-β-Dp does not enthalpically discriminate between the 5′-TGGTA-3′ match site and the 5′-TGTTA-3′ single mismatch site. The same structural explanations presented above to account for the similarity in ImImPy-γ-PyPyPy-β-Dp affinity for the 5′-TGGTA-3′ and 5′-TGTTA-3′ sites can be used here to explain the inability of the hairpin polyamide to discriminate enthalpically between these two sites.

Table 2: Calorimetrically Derived Binding Enthalpies (ΔH_b) for the Interactions of ImImPy-γ-PyPyPy-β-Dp with the Three 11-mer DNA Duplexes at 20 °C[a]

duplex	ΔH_b[b] (kcal/mol)
1 (5′-TGTTA-3′)	−6.6 ± 0.8
2 (5′-TGGTA-3′)	−6.9 ± 0.8
3 (5′-TATTA-3′)	−1.3 ± 0.7

[a] Solution conditions are as described in the footnote to Table 1. [b] ΔH_b values were determined at a [total ligand] to [duplex] ratio (r_{Dup}) of 1.0, with the indicated uncertainties corresponding to the sum of the standard deviations from three separate mixing experiments (DNA−ligand, ligand−buffer, and buffer−buffer) of at least 18 independent injections each.

Table 3: ΔT_m-Derived Binding Affinities of ImImPy-γ-PyPyPy-β-Dp for the Three 11-mer DNA Duplexes at 20 °C[a]

duplex	T_m°[b] (°C)	T_m[b] (°C)	$K_{20}^{\Delta T_m}$[c] (M^{-1})
1 (5′-TGTTA-3′)	42.7 ± 0.3	48.9 ± 0.5	(1.1 ± 0.4) × 10^7
2 (5′-TGGTA-3′)	46.1 ± 0.3	54.9 ± 0.5	(3.0 ± 1.0) × 10^7
3 (5′-TATTA-3′)	38.1 ± 0.3	39.2 ± 0.3	(1.9 ± 1.3) × 10^5

[a] Solution conditions are as described in the footnote to Table 1. [b] T_m values were derived from UV melting profiles at 5 μM duplex (D) in the absence (T_m°) and presence of ligand (L) at a stoichiometric ratio of 1L/1D. Each T_m value is an average derived from at least two independent experiments, with the indicated errors corresponding to the average deviation from the mean. [c] Binding constants at 20 °C ($K_{20}^{\Delta T_m}$) were determined using eqs 2 and 3, the appropriate values of ΔH_b listed in Table 2, and the following calorimetrically determined (*17*) duplex-to-single strand transition enthalpies (ΔH_{WC}) for the three host duplexes: 77.1 kcal/mol for duplex **1**, 73.5 kcal/mol for duplex **2**, and 60.1 kcal/mol for duplex **3**. The indicated uncertainties reflect the maximum errors in $K_{20}^{\Delta T_m}$ that result from the corresponding uncertainties noted above in T_m and T_m°, as propagated through eqs 2 and 3.

Further inspection of the data in Table 2 reveals that ImImPy-γ-PyPyPy-β-Dp binding to duplex **3**, which contains the 5′-TATTA-3′ double mismatch site, is less enthalpically favorable than binding to either the 5′-TGGTA-3′ match site of duplex **2** or the 5′-TGTTA-3′ single mismatch site of duplex **1**. This observation also may be interpreted using the structural framework provided by the NMR study described above (*19*). To be specific, when the ImImPy-γ-PyPyPy-β-Dp ligand complexes with the 5′-TATTA-3′ double mismatch site of duplex **3**, it should be unable to form either of the two imidazole(N)−(amino H2)guanine hydrogen bonds which it can form when the ligand is complexed with the 5′-TGGTA-3′ match site. This loss of two hydrogen bonds, at best, might partially be compensated by formation of a single amide−(O2)thymine hydrogen bond. However, a lack of conformational flexibility may render the ImImPy-γ-PyPyPy-β-Dp ligand unable to form even this hydrogen bond. The inability of ImImPy-γ-PyPyPy-β-Dp to

Table 4: Thermodynamic Parameters for the Binding of ImImPy-γ-PyPyPy-β-Dp to the Three 11-mer DNA Duplexes[a]

duplex	ΔH_b[b] (kcal/mol)	$T\Delta S_b$[c] (kcal/mol)	ΔG_{b-20}[d] (kcal/mol)	$K_{20}^{\Delta T_m}$ [b]
1 (5′-TGTTA-3′)	−6.6 ± 0.8	+2.8 ± 1.0	−9.4 ± 0.2	(1.1 ± 0.4) × 10^7
2 (5′-TGGTA-3′)	−6.9 ± 0.8	+3.1 ± 1.0	−10.0 ± 0.2	(3.0 ± 1.0) × 10^7
3 (5′-TATTA-3′)	−1.3 ± 0.7	+5.8 ± 1.0	−7.1 ± 0.3	(1.9 ± 1.3) × 10^5

[a] Solution conditions are as described in the footnote to Table 1. [b] The indicated errors in ΔH_b and $K_{20}^{\Delta T_m}$ are as described in the footnotes to Tables 2 and 3, respectively. [c] ΔS_b is the binding entropy, as determined using eq 5 in the text and the corresponding values of ΔH_b and ΔG_{b-20}. The indicated uncertainties reflect the maximum possible errors in ΔS_b that result from the corresponding uncertainties noted above in ΔH_b and ΔG_{b-20}, as propagated through eq 5. [d] ΔG_{b-20} is the binding free energy at 20 °C, as determined using eq 4 in the text and the corresponding value of $K_{20}^{\Delta T_m}$. The indicated uncertainties reflect the errors in ΔG_{b-20} that result from the corresponding uncertainties noted above in $K_{20}^{\Delta T_m}$, as propagated through eq 4.

compensate for the loss of two imidazole(N)−(amino H2)-guanine hydrogen bonds when complexed with the 5′-TATTA-3′ double mismatch site may give rise to its reduced binding enthalpy relative to that which it exhibits when complexed with the 5′-TGGTA-3′ match site. Independent of the veracity of such microscopic interpretations of the macroscopic data, our results provide a dramatic example of the dangers of assuming a simple additivity approach for predicting the thermodynamic impact of mispairings in polyamide−DNA interactions. It appears that, at least for the polyamide−DNA system studied here, *a single mismatch site can more readily be energetically accommodated than a double mismatch site*.

Apparent Binding Affinities Derived from Analysis of Ligand-Induced Changes in Duplex Thermal Stability (ΔT_m) Are Consistent with Those Derived from the Fitting of Induced CD Titration Profiles. In addition to the CD analysis described above, we have used the ΔT_m approach described below to assess independently the relative strength of ImImPy-γ-PyPyPy-β-Dp binding to the three duplexes. Measured ligand-induced changes in the thermal stabilities of each of the three 11-mer duplexes (see Figure 2 and Table 3) were used to estimate apparent ligand−duplex association constants at T_m (K_{T_m}) from the following expression (*28*):

$$\frac{1}{T_m^\circ} - \frac{1}{T_m} = \frac{nR}{(\Delta H_{dup})} \ln[1 + (K_{T_m})a_f] \qquad (2)$$

where T_m° and T_m are the melting temperatures of the ligand-free and ligand-saturated duplexes, respectively; n is the number of ligand binding sites on the duplex (a value we estimate as one based on the CD results described above); ΔH_{dup} is the enthalpy change for the melting of a duplex in the absence of bound ligand [values we previously determined for each duplex (*17*) using DSC]; and a_f is the free ligand activity at T_m (a value we estimate as one-half $[L]_T$). The K_{T_m} values calculated in this manner were extrapolated to a common reference temperature of 20 °C using the binding enthalpies (ΔH_b) listed in Table 2 and the van't Hoff relationship:

$$\frac{\partial(\ln K)}{\partial\left(\frac{1}{T}\right)} = -\frac{\Delta H_b}{R} \qquad (3)$$

The resulting K values are listed in Table 3. Inspection of these data reveals the ΔT_m-derived K values to be in good agreement with the corresponding CD-derived K values listed in Table 1, an observation that validates the use of either the ΔT_m or the CD titration curve-fitting approach for deriving ligand−duplex association constants. Note that both methods are consistent in revealing the preferential binding of ImImPy-γ-PyPyPy-β-Dp to the 5′-TGGTA-3′ match and 5′-TGTTA-3′ single mismatch sites relative to the 5′-TATTA-3′ double mismatch site, although the magnitude of the observed differential binding is somewhat higher using the ΔT_m method.

Table 5: Thermodynamic Consequences of Single and Double Base Pair Changes on the Binding of ImImPy-γ-PyPyPy-β-Dp to the 5′-TGGTA-3′ Match Site

duplex	$\Delta\Delta H_b$[a] (kcal/mol)	$\Delta(T\Delta S_b)$[a] (kcal/mol)	$\Delta\Delta G_{b-20}$[a] (kcal/mol)
1 (5′-TGTTA-3′)	+0.3	−0.3	+0.6
2 (5′-TGGTA-3′)	−	−	−
3 (5′-TATTA-3′)	+5.6	+2.7	+2.9

[a] $\Delta\Delta H_b$, $\Delta(T\Delta S_b)$, and $\Delta\Delta G_{b-20}$ were determined by subtracting the values of ΔH_b, $T\Delta S_b$, and ΔG_{b-20} for duplex **2** from the corresponding ΔH_b, $T\Delta S_b$, and ΔG_{b-20} values for either duplex **1** or duplex **3**.

Thermodynamic Origins of the Binding Affinities of ImImPy-γ-PyPyPy-β-Dp: Ligand Binding at 20 °C to the Match Site and to the Single Mismatch Site is Enthalpy-Driven, While Ligand Binding to the Double Mismatch Site is Entropy-Driven. Armed with the binding constants listed in Table 3, we have calculated the corresponding binding free energies (ΔG_b) using the standard relationship:

$$\Delta G_b = -RT \ln K \qquad (4)$$

These binding free energies, coupled with our calorimetrically determined binding enthalpies, allow us to calculate the corresponding binding entropies (ΔS_b) using the standard relationship:

$$\Delta S_b = \frac{\Delta H_b - \Delta G_b}{T} \qquad (5)$$

These calculations enabled us to generate complete thermodynamic profiles for the binding of ImImPy-γ-PyPyPy-β-Dp to each of the three 11-mer DNA duplexes studied here. The resulting profiles are summarized in Table 4. Inspection of these data reveals the binding of the hairpin polyamide at 20 °C to the 5′-TGGTA-3′ match site of duplex **2** and to the 5′-TGTTA-3′ single mismatch site of duplex **1** to be primarily (∼70%) enthalpy-driven. By contrast, the binding of ImImPy-γ-PyPyPy-β-Dp to the 5′-TATTA-3′ double mismatch site of duplex **3** is primarily (∼82%) entropy-driven. This favorable entropic contribution may reflect binding-induced desolvation of the all-AT minor groove that is present only in duplex **3** (*30*−*32*). Note that the reduced

Table 6: Thermodynamic Comparison of ImImPy-γ-PyPyPy-β-Dp (ImIm) and ImPyPy-γ-PyPyPy-β-Dp (ImPy) Binding to the Three 11-mer DNA Duplexes[a]

	ΔH_b (kcal/mol)		$T\Delta S_b$ (kcal/mol)		ΔG_{b-20} (kcal/mol)		$K_{20}^{\Delta T_m}$ (M^{-1})	
duplex	ImIm	ImPy	ImIm	ImPy[b]	ImIm	ImPy[b]	ImIm	ImPy[b]
1 (5′-TGTTA-3′)	-6.6 ± 0.8	-6.7 ± 0.6	$+2.8 \pm 1.0$	$+4.0 \pm 0.8$	-9.4 ± 0.2	-10.7 ± 0.2	$(1.1 \pm 0.4) \times 10^7$	$(8.0 \pm 3.7) \times 10^7$
2 (5′-TGGTA-3′)	-6.9 ± 0.8	-4.6 ± 0.8	$+3.1 \pm 1.0$	$+3.4 \pm 1.1$	-10.0 ± 0.2	-8.0 ± 0.3	$(3.0 \pm 1.0) \times 10^7$	$(9.1 \pm 5.7) \times 10^5$
3 (5′-TATTA-3′)	-1.3 ± 0.7	-4.4 ± 0.6	$+5.8 \pm 1.0$	$+4.4 \pm 0.7$	-7.1 ± 0.3	-8.8 ± 0.1	$(1.9 \pm 1.3) \times 10^5$	$(3.3 \pm 1.1) \times 10^6$

[a] Solution conditions are as described in the footnote to Table 1. [b] $T\Delta S_b$, ΔG_{b-20}, and $K_{20}^{\Delta T_m}$ values for ImPy binding supersede those values previously reported (*17*).

binding to the 5′-TATTA-3′ site of duplex **3** results from a less favorable binding enthalpy. In fact, relative to duplexes **2** and **1**, the reduced binding to duplex **3** occurs despite a favorable entropic contribution to binding [$\Delta(T\Delta S)$], which is overcompensated by a substantially less favorable binding enthalpy. Thus, relative to the double mismatch site, the preferential binding of ImImPy-γ-PyPyPy-β-Dp to the 5′-TGGTA-3′ and 5′-TGTTA-3′ sites is *enthalpic in origin.*

The Differential DNA-Binding Affinities of the ImImPy-γ-PyPyPy-β-Dp Hairpin Polyamide Are Entirely Enthalpic in Origin. The data listed in Table 4 allow us to evaluate by differences the thermodynamic consequences on ImImPy-γ-PyPyPy-β-Dp binding of single or double base pair changes in the 5′-TGGTA-3′ match site. The resulting differential data are listed in Table 5. Inspection of these data reveals that the single base pair change in duplex **2** that produces duplex **1** (a G·C to T·A conversion at position 3) results in negligible changes in binding enthalpy and entropy. In other words, the 5′-TGGTA-3′ to 5′-TGTTA-3′ single base pair change has a negligible thermodynamic impact on ImImPy-γ-PyPyPy-β-Dp binding. Further inspection of the data in Table 5 reveals that the double base pair change in duplex **2** that produces duplex **3** (a G·C to A·T conversion at position 2 and a G·C to T·A conversion at position 3) results in a 5.6 kcal/mol loss of binding enthalpy (ΔH_b) and a 2.7 kcal/mol gain in the entropic contribution to binding ($T\Delta S_b$), which only partially compensates the loss in binding enthalpy. These enthalpy and entropy changes translate into a loss in binding free energy of 2.9 kcal/mol. *Thus, the 2.3−2.9 kcal/mol enhanced affinity exhibited by ImImPy-γ-PyPyPy-β-Dp for the 5′-TGGTA-3′ and 5′-TGTTA-3′ sites relative to the 5′-TATTA-3′ double mismatch site is entirely enthalpic in origin.*

Thermodynamic Comparison of ImImPy-γ-PyPyPy-β-Dp and ImPyPy-γ-PyPyPy-β-Dp Binding to the Three DNA Duplex Sites. Table 6 presents a comparison of the thermodynamic parameters for the binding of two hairpin polyamides, ImImPy-γ-PyPyPy-β-Dp and ImPyPy-γ-PyPyPy-β-Dp, to the three DNA duplex binding sites studied here. The $T\Delta S_b$, ΔG_{b-20}, and K values for ImPyPy-γ-PyPyPy-β-Dp binding listed in this table supersede those previously reported, although the relative rank and associated conclusions remain unchanged.

Inspection of the data in Table 6 reveals a number of features worthy of note. First, the highest-affinity site for ImImPy-γ-PyPyPy-β-Dp is 5′-TGGTA-3′ (duplex **2**), while the highest-affinity site for ImPyPy-γ-PyPyPy-β-Dp is 5′-TGTTA-3′ (duplex **1**). These observations are consistent with previous footprinting studies and with the Dervan "paring rules" that govern Py-Im polyamide recognition of duplex DNA (*1*−*5*). Note that the association constants we observe for the binding of ImPyPy-γ-PyPyPy-β-Dp to its 5′-TGTTA-3′ match site [$(8.0 \pm 3.7) \times 10^7$ M^{-1}] and for the binding of ImImPy-γ-PyPyPy-β-Dp to its 5′-TGGTA-3′ match site [$(3.0 \pm 1.0) \times 10^7$ M^{-1}] are in good agreement with the corresponding values [$(7.6 \pm 0.8) \times 10^7$ and 9.0×10^7 M^{-1}, respectively] derived from footprinting results (*12*−*14*). Thus, both footprinting and optical/calorimetric studies independently result in similar association constants for ImPyPy-γ-PyPyPy-β-Dp and ImImPy-γ-PyPyPy-β-Dp binding to their designated match sites. This agreement not only is gratifying, but also suggests that oligomeric hosts provide good models for ligand binding to more heterogeneous polymeric targets, thereby validating the assumption of independent sites used in the analysis of the footprinting data (*33*).

A second feature that emerges from the data (Table 6) is that both ImImPy-γ-PyPyPy-β-Dp and ImPyPy-γ-PyPyPy-β-Dp enthalpically favor their designated match sites (5′-TGGTA-3′ and 5′-TGTTA-3′, respectively) over the 5′-TATTA-3′ site in duplex **3**, which possesses an unobstructed (all-AT) minor groove. Interestingly, both ligands exhibit the most favorable entropic contributions to binding when they complex with the 5′-TATTA-3′ site. However, the binding affinities of both hairpin polyamides for the 5′-TATTA-3′ site are lower than for their match sites due to significantly less favorable binding enthalpies.

A third feature that emerges from the data in Table 6 is that ImPyPy-γ-PyPyPy-β-Dp exhibits greater enthalpic (+2.1 to +2.3 kcal/mol) and free energy discrimination (+1.9 to +2.7 kcal/mol) between its match site and single mismatch site(s) than does ImImPy-γ-PyPyPy-β-Dp ($\Delta\Delta H_b = +0.3$ kcal/mol and $\Delta\Delta G_{b-20} = +0.6$ kcal/mol). *While a Py → Im change in ImPyPy-γ-PyPyPy-β-Dp to form the ImImPy-γ-PyPyPy-β-Dp ligand increases binding affinity for the match site (5′-TGGTA-3′), it reduces the binding selectivity for the match site relative to the single mismatch site.*

The comparisons reported here are minimum first steps toward establishing the thermodynamic database needed to provide insight into the molecular forces that govern polyamide recognition of duplex DNA, including the data required to design rationally hairpin polyamides with predictable sequence-dependent DNA affinities and specificities. In this regard, Py-Im polyamides have been shown to inhibit specific transcription of genes in cell culture by binding to specific promoter sequences (*34*, *35*). Consequently, predictable binding affinities and specificities using the pairing rules for predetermined DNA sites would have enormous value. A key next step is to characterize the thermodynamics of the Hp/Py pair at T·A, which will be reported in due course.

REFERENCES

1. Wade, W. S., Mrksich, M., and Dervan, P. B. (1992) *J. Am. Chem. Soc. 114*, 8783−8794.
2. Mrksich, M., and Dervan, P. B. (1993) *J. Am. Chem. Soc. 115*, 2572−2576.
3. Pelton, J. G., and Wemmer, D. E. (1989) *Proc. Natl. Acad. Sci. U.S.A. 86*, 5723−5727.
4. White, S., Baird, E. E., and Dervan, P. B. (1996) *Biochemistry 35*, 12532−12537.
5. White, S. E., Szewczyk, J. W., Turner, J. M., Baird, E. E., and Dervan, P. B. (1998) *Nature 391*, 468−471.
6. Mrksich, M., Wade, W. S., Dwyer, T. J., Geierstanger, B. H., Wemmer, D. E., and Dervan, P. B. (1992) *Proc. Natl. Acad. Sci. U.S.A. 89*, 7586−7590.
7. Geierstanger, B. H., Dwyer, T. J., Bathini, Y., Lown, J. W., and Wemmer, D. E. (1993) *J. Am. Chem. Soc. 115*, 4474−4482.
8. Geierstanger, B. H., Mrksich, M., Dervan, P. B., and Wemmer, D. E. (1994) *Science 266*, 646−650.
9. Chen, X., Ramakrishnan, B., Rao, S. T., and Sundaralingam, M. (1994) *Struct. Biol. 1*, 169−175.
10. Kielkopf, C. L., Baird, E. E., Dervan, P. B., and Rees, D. C. (1998) *Nat. Struct. Biol. 5*, 104−109.
11. Kielkopf, C. L., White, S. E., Szewczyk, J. W., Turner, J. M., Baird, E. E., Dervan, P. B., and Rees, D. C. (1999) *Science* (in press).
12. Mrksich, M., Parks, M. E., and Dervan, P. B. (1994) *J. Am. Chem. Soc. 116*, 7983−7988.
13. Parks, M. E., Baird, E. E., and Dervan, P. B. (1996) *J. Am. Chem. Soc. 118*, 6147−6152.
14. Parks, M. E., Baird, E. E., and Dervan, P. B. (1996) *J. Am. Chem. Soc. 118*, 6153−6159.
15. Swalley, S. E., Baird, E. E., and Dervan, P. B. (1996) *J. Am. Chem. Soc. 118*, 8198−8206.
16. Trauger, J. W., Baird, E. E., and Dervan, P. B. (1996) *Nature 382*, 559−561.
17. Pilch, D. S., Poklar, N., Gelfand, C. A., Law, S. M., Breslauer, K. J., Baird, E. E., and Dervan, P. B. (1996) *Proc. Natl. Acad. Sci. U.S.A. 93*, 8306−8311.
18. White, S., Baird, E. E., and Dervan, P. B. (1997) *J. Am. Chem. Soc. 119*, 8756−8765.
19. de Clairac, R. P. L., Geierstanger, B. H., Mrksich, M., Dervan, P. B., and Wemmer, D. E. (1997) *J. Am. Chem. Soc. 119*, 7909−7916.
20. Griswold, B. L., Humoller, F. L., and McIntyre, A. R. (1951) *Anal. Chem. 23*, 192−194.
21. Baird, E. E., and Dervan, P. B. (1996) *J. Am. Chem. Soc. 118*, 6141−6146.
22. Marky, L. A., and Breslauer, K. J. (1987) *Biopolymers 26*, 1601−1620.
23. Breslauer, K. J. (1995) *Methods Enzymol. 259*, 221−242.
24. Mudd, C. P., and Berger, R. L. (1988) *J. Biochem. Biophys. Methods 17*, 171−192.
25. Remeta, D. P., Mudd, C. P., Berger, R. L., and Breslauer, K. J. (1991) *Biochemistry 30*, 9799−9809.
26. Robinson, A. L. (1932) *J. Am. Chem. Soc. 54*, 1311−1318.
27. Gulbransen, E. A., and Robinson, A. L. (1934) *J. Am. Chem. Soc. 56*, 2637−2641.
28. Crothers, D. M. (1971) *Biopolymers 10*, 2147−2160.
29. Snyder, J. G., Hartman, N. G., D'Estantoit, B. L., Kennard, O., Remeta, D. P., and Breslauer, K. J. (1989) *Proc. Natl. Acad. Sci. U.S.A. 86*, 3968−3972.
30. Drew, H. R., and Dickerson, R. E. (1981) *J. Mol. Biol. 151*, 535−556.
31. Kopka, M. L., Yoon, C., Goodsell, D., Pjura, P., and Dickerson, R. E. (1985) *Proc. Natl. Acad. Sci. U.S.A. 82*, 1376−1380.
32. Marky, L. A., and Breslauer, K. J. (1987) *Proc. Natl. Acad. Sci. U.S.A. 84*, 4359−4363.
33. Brenowitz, M., Senear, D. F., Shea, M. A., and Ackers, G. K. (1986) *Methods Enzymol. 130*, 132−181.
34. Gottesfield, J. M., Nealy, L., Trauger, J. W., Baird, E. E., and Dervan, P. B. (1997) *Nature 387*, 202−205.
35. Dickenson, L. A., Guzilia, P., Trauger, J. W., Baird, E. E., Mosier, D. M., Gottesfeld, J. M., and Dervan, P. B. (1998) *Proc. Natl. Acad. Sci. U.S.A. 95*, 12890−12895.

BI982628G